

---

---

ELECTRICAL  
AND MAGNETIC PROPERTIES

---

---

## Effect of Residual Internal Stresses in TiN Coatings on Specific Losses in Anisotropic Electrical Steel

A. A. Solov'ev, N. S. Sochugov, and K. V. Oskomov

*Institute of High-Current Electronics, Siberian Branch, Russian Academy of Sciences,  
pr. Akademicheskii 23, Tomsk, 634055 Russia*

Received April 9, 2008

**Abstract**—Methods of X-ray diffraction analysis, mass-spectrometry, and atomic-force microscopy have been used to perform a comparative analysis of factors that cause the appearance of residual stresses in TiN coatings deposited by reactive magnetron sputtering and to study their effect on specific magnetic losses in electrical-sheet steel. Physical and mechanical parameters of coatings, such as hardness, elastic modulus, residual stress, microstructure, and surface morphology, have been studied. It has been shown that the level of internal stresses in a coating depends on its thickness and increases with increasing quantity and energy of ions in the deposited beam. The maximum magnitudes of compressive stresses in coatings (13 GPa) were obtained when using an unbalanced working regime of the magnetron and a negative bias at the substrate. The hardness of coatings produced under such conditions reaches 29 GPa. There has been demonstrated a possibility of reducing losses in electrical-sheet steels by about 15% by depositing surface coatings with high compressive stresses.

*Key words:* magnetron sputtering, coatings, electrical steel, internal stresses, ion bombardment

**DOI:** 10.1134/S0031918X1002002X

### INTRODUCTION

An increase in the power generation leads to an increase in the electrical-sheet steel production. Modern cold-rolled anisotropic electrical steel (AESs) are mainly used for manufacturing magnetic circuits for power transformers and other products of electrical industry. The quality of steels of this class is determined by a number of properties, which depend on the concentration of silicon, type and intensity of a crystal texture, perfection of the crystal lattice, grain size, quantity of inclusions and degree of their dispersity, internal stresses, sheet thickness, and the condition of the sheet surface. The modern AESs have a coarse grain with sharp cube-on-edge texture (110)[001], with an easy axis [001] oriented along the rolling direction, which provides high service properties of the steel. Specific magnetic losses  $P_{1.7/50}$  (at the induction of 1.7 T and the frequency of magnetization reversal of 50 Hz) appear to be one of the main rated parameters of the quality of the electrical-sheet steel [1].

At present, at the final stages of AES production, there are carried out treatments which improve magnetic properties of a steel. Such methods include, for example, depositing magnetoactive insulating coatings that induce the formation of oriented internal stresses, creating local structural surface barriers by laser or another type of treatments, which affect the size and shape of grains, and the type of the magnetic domain structure [1–5]. The efficiency of such tech-

nological operations is determined by the magnitude of changes in the magnetic properties before and after the treatment.

This work was aimed at determining the effect of properties of thin-film coatings, which are being deposited at final stages of AES production and create tensile stresses in the steel, on the changes in the level of magnetic losses in the steel. Specific power losses are one of the main characteristics that are used for the evaluation of the quality of this material.

The influence of elastic stresses in AES on its magnetic properties has long been known [6]. The formation of coatings with high compressive stresses (on the order of a few GPa) leads to the appearance of tensile stresses in a substrate, which are by orders of magnitude lower (to 25 MPa) depending on the film-to-substrate thickness ratio. Such coatings can be produced using metal carbide or nitride films (TiN, BN, ZrN, AlN, TiC, ZrC, WC) and amorphous carbon films [7]. These coatings are able to create tensile stresses in a substrate and, due to improving a domain structure of the steel, to decrease specific magnetic losses.

On the one hand, high residual stresses in coatings often lead to their separation from a substrate during exploitation. On the other hand, as is known, the wear-resistant coatings are working better under the condition of relatively high compressive stresses, which prevent from the development of fatigue cracks. Residual stresses in coatings can appear due to differ-

ent reasons. One of these is the difference between the thermal expansion coefficients of a substrate and a coating. Therefore, the magnitude of thermal stresses depends on a substrate temperature during coating deposition. The magnitude of residual thermal stresses can be estimated by the formula [8]

$$\sigma_T = \frac{E_f}{1 - \nu_f} (\alpha_f - \alpha_s) (T_D - T_M), \quad (1)$$

where  $E_f$  is the average elastic modulus of the coating in the temperature range  $\Delta T$ ;  $\nu_f$  is Poisson's ratio for the material of the coating;  $\alpha_s$  and  $\alpha_f$  are the thermal expansion coefficients of the substrate and a coating, respectively;  $T_D$  is the temperature of the film deposition; and  $T_M$  is the temperature upon which stresses in the coating were measured.

As follows from formula (1), carbides and nitrides with high magnitudes of Young's moduli and low magnitudes of thermal expansion coefficients are the most appropriate materials for substrate-stretching coatings. For example, Yamaguchi et al. [9] have studied the effect of TiN coatings applied by the method of high-temperature chemical gas-phase deposition on the magnetic losses in a grain-oriented electrical steel.

Another factor that can cause the formation of residual stresses is internal stresses in the coating, which appear in the result of bombardment of a growing film by high-energy particles. Such bombardment is typical of the ion-assisted methods of deposition. In the case of magnetron sputtering, such particles can be neutral atoms scattered from the cathode, ions of a working gas (Ar) that are generated in the discharge, and neutralized ions reflected from the cathode [10]. Although the majority of Ar ions that bombard the cathode to be sputtered are become neutralized on it, part of ions reflects from the cathode as a result of elastic collisions.

The total residual stresses in coatings appear to be a sum of thermal and internal stresses:

$$\sigma = \sigma_T + \sigma_I. \quad (2)$$

As a rule, the residual stresses in coatings deposited by magnetron sputtering, appear to be compressive and are due to distortions produced in the crystal lattice of a growing film by high-energy particles. The magnitude of internal stresses depends on the properties of a deposited material, which are characterized by a coefficient  $Q$  [10]

$$Q = \frac{EM}{(1 - \nu)D}, \quad (3)$$

where  $E$  is the elasticity modulus,  $M$  is the atomic mass,  $D$  is the density, and  $\nu$  is Poisson's ratio of the deposited material.

For example, the magnitudes of these characteristics for AlN are  $Q = 5.5 \times 10^3$  J/mol and  $\sigma = -3$  GPa [10].

In this work we have carried out an analysis of the effect of TiN coatings with residual compressive stresses on the level of magnetic losses in the electri-

cal-sheet steel and have determined the optimum conditions for coating deposition, which lead to the largest decrease in these energy losses.

## EXPERIMENTAL

The deposition of coatings was carried out in a setup with a vacuum chamber with dimensions  $600 \times 600 \times 600$  mm made of a stainless steel, using a magnetron sputtering system, whose construction and plasma characteristics were described in [11]. The coatings were applied onto substrates of electrical steel and of silicon, which were located at a distance of 12 cm from the magnetron. For our experiments we have used cold-rolled anisotropic electrical steel of grade 3405 in the form of strips  $50 \times 150$  mm in size and 0.35 mm thick (produced from an Fe–3 wt % Si alloy). Before depositing a TiN coating, the insulating coating was removed from the surface of the sample. The flow rate of Ar in the experiments was maintained constant at a level of  $68 \text{ cm}^3/\text{min}$ . The total working pressure in the chamber did not exceed 0.15 Pa and depended on the consumption of nitrogen, which varied from 10 to  $17 \text{ cm}^3/\text{min}$ . The discharge power was constant and was equal to 1.5 kW. The controlled parameters, the effect of which on the properties of coatings was investigated in this work, were the partial pressure of nitrogen, the current in the disbalancing magnetron coil, and the bias voltage at the substrate.

The temperature of the samples during coating deposition was measured with a help of a chromel–alumel thermocouple with acceptable deviation of indications in the temperature range used equal to  $\pm 0.16$  mV. The thickness of coatings was measured by a MII-4 microinterferometer. The study of the phase composition and structural parameters of TiN coatings on Si substrates was carried out on an XRD-60 diffractometer using  $\text{CuK}\alpha$  radiation. An analysis of the samples was performed using an asymmetrical Bragg–Brentano scheme with an angular scanning in steps of  $\alpha = 5^\circ$ . The hardness and the elasticity modulus of the films obtained were measured using a NanoTest 100 nanoindenter. The load at the indenter was no more than 5 mN, so that the depth of its penetration into the coating did not exceed 10% of the coating thickness. In each case, there was obtained from 5 to 10 indentations at the sample for calculating average magnitudes of the measured parameters. Besides, there was carried out a control of the coating morphology with the help of a Solver P47 atomic-force microscope. For this type of studies, the coatings were deposited onto substrates of a polished silicon.

Magnetic losses were measured on a setup for measuring magnetic properties of strip-shaped samples by the method of wattmeter and ammeter according to the Russian Standard GOST 12119.4-98. For this purpose, TiN coatings were deposited onto samples of anisotropic electrical steel of grade 3405 0.35 mm thick with specific magnetic losses  $P_{1.7/50} = 1.44\text{--}1.5$  W/kg accord-

**Table 1.** Dependence of the characteristics of TiN coatings on the deposition parameters (Si substrate)

No.	$Q_{Ar}$ , cm <sup>3</sup> /min	$Q_{N_2}$ , cm <sup>3</sup> /min	$d$ , nm	$H$ , GPa	$E$ , GPa	$a$ , Å	CD, nm	$\Delta d/d \times 10^3$	$I$ , %	$hkl$	$\sigma$ , GPa
1K	68	10	1815	19.8	292	4.2392	15	2.7	52	111	2.71
2K	68	12	1865	22.1	295	4.2424	12	0.55	34	111	0.55
3K	68	14	1570	17.5	281	4.2500	16	2.1	43	111	2.03
4K	68	16	1330	18.3	236	4.2555	16	5.5	31	100	4.47
5K	68	18	1065	24.4	261	4.2302	13	2.5	48	100	2.25
6K	68	16	370	–	–	4.2155	10	3.8	42	100	3.14
7K	68	16	720	–	–	4.2638	11	2.3	50	111	1.9
8K	68	16	815	–	–	4.2580	20	6.4	71	110	5.3
9K	68	16	860	–	–	4.2388	19	7.2	70	111	5.96

Note:  $Q$ , the gas flow rate;  $d$ , coating thickness;  $H$ , coating hardness;  $E$ , elasticity modulus; CD, coherent domain;  $\Delta d/d$ , microdeformations;  $I$ , relative intensity of peaks in X-ray diffraction patterns;  $hkl$ , planes of preferred orientation; and  $\sigma$ , internal stresses.

ing to GOST 21427.1-87. The results of measurements of magnetic losses were averaged over three samples processed by the same regime.

The internal stresses in the coatings were measured by two methods. In the case of silicon substrates, the X-ray diffraction method was used. In this case, the deformation of the film material is determined directly under the condition that its elasticity limit is not achieved, i.e., Hooke's law is satisfied, so that we have [12]

$$\sigma = \frac{E_f d_0 - d}{2\nu_f d_0}, \quad (4)$$

where  $\nu_f$  is Poisson's ratio of the film material ( $\nu_{TiN} = 0.29$  [13]),  $E_f$  is Young's modulus of the film,  $d_0$  is the equilibrium interplanar spacing, and  $d$  is the interplanar spacing in the film with stresses. For substrates of electrical steel, the residual stresses were determined from the change in the radius of curvature of the substrate measured before and after deposition of the coating by the formula [10]

$$\sigma = \frac{E_s d_s^2}{6(1 - \nu_s) d_f} \left( \frac{1}{R_2} - \frac{1}{R_1} \right), \quad (5)$$

where  $E_s/(1 - \nu_s)$  is the elasticity modulus of the substrate;  $d_s$  and  $d_f$  are the thicknesses of the substrate and the film, respectively; and  $R_1$  and  $R_2$  are the radii of curvature of the substrate before and after deposition of the coating, respectively.

To study the effect of ion bombardment during deposition of TiN coatings on the level of residual stresses in the films, we measured, using a 45° HIDEN EQP electrostatic analyzer, the energy spectra of positive ions in a magnetron discharge. The measuring device was placed at the axis of the magnetron at a dis-

tance of 13.5 cm from its cathode. The orifice through which the ions of the discharge plasma were extracted had a diameter of 0.1 mm.

## RESULTS AND DISCUSSION

As a material of coatings, we chose titanium nitride as the wear-resistant material most studied and widely applied in industry for surface protection. As is known, the homogeneity field of TiN in the Ti–N phase diagram is very wide; therefore, its properties depend on the quantity of nitrogen in the nitride. Upon a high deposition rate, there can be obtained a fine-grained and, subsequently, highly distorted structure with metastable phases; whereas upon low deposition rates, there is formed a flaked structure. The microhardness of TiN films varies in wide limits (from 20 to 40 GPa) depending on the nitrogen amount and structural peculiarities. The large hardness of the condensed TiN is a consequence of the high level of internal stresses. The coatings produced by the methods of physical gas-phase deposition often have internal compressive stresses on the level of  $10^9$ – $10^{10}$  Pa. The presence of such stresses is testified by an increase of the lattice parameter ( $a$ ). For stoichiometric films, there is often reported a magnitude  $a = 0.425$  nm (for a stoichiometric bulk TiN,  $a = 0.424$  nm). The magnitude of the lattice parameter is determined by a number of factors; e.g., an increase in  $a$  can be caused by an increase in the N concentration in the crystal lattice, by a decrease in the film thickness, or by a growth of internal stresses [14].

The properties of the TiN coatings on Si substrates produced in our experiments are shown in Table 1. To achieve the main goal of this work, i.e., a decrease in specific losses in a transformer steel, we had to obtain

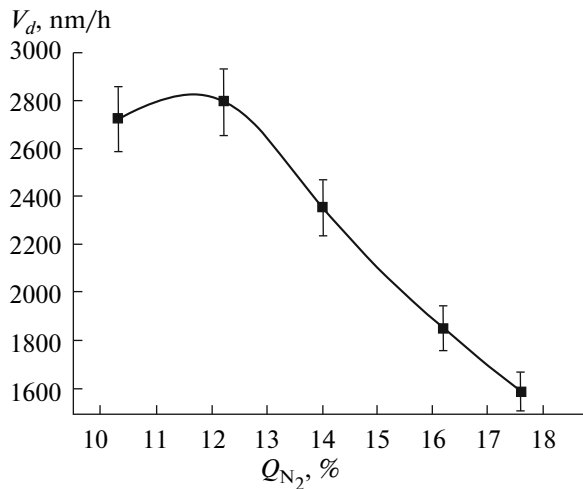


**Fig. 1.** Dependence of the rate of deposition of TiN coatings  $V_d$  on the nitrogen flow rate  $Q_{N_2}$  ( $Q_{Ar} = 68 \text{ cm}^3/\text{min}$ ; the discharge power is 1.5 kW).

coatings with highest internal stresses, so that their effect be maximum. At the same time, it was necessary to prevent fracture of the coating or its separation from the substrate.

At the first stage, we have measured properties of coatings depending on the nitrogen flow rate. The consumption of Ar was maintained constant at a level of  $68 \text{ cm}^3/\text{min}$ . As was expected, addition of  $N_2$  to the working chamber led to a decrease in the TiN deposition rate with increasing N consumption (Fig. 1). It is caused by “poisoning” of the sputtered cathode, i.e., by the formation of a dielectric film with a sputtering ratio less than that of pure Ti, on its surface.

It is known [15] that for depositing stoichiometric TiN coatings by the method of reactive sputtering in an Ar+N<sub>2</sub> mixture the partial pressure of nitrogen should be equal to 17% of the total pressure in the chamber. In our case, such ratio of partial pressures was observed at  $Q_{N_2} = 16 \text{ cm}^3/\text{min}$ . Upon such a flow rate of nitrogen, there were also observed largest residual stresses in the coatings (4.41 GPa). Therefore, all subsequent experiments were carried out with  $Q_{N_2} = 16 \text{ cm}^3/\text{min}$ .

Depending on the nitrogen flow rate, the TiN coatings had a nanohardness  $H$  from 18 to 25 GPa at the elasticity modulus  $E$  from 240 to 290 GPa (Table 1). It is known that the hardness of the coating depends on the partial pressure of the reactive gas, the substrate temperature, and the voltage at the substrate. Depending on the parameters of the process upon the magnetron sputtering, the TiN<sub>*x*</sub> (*x* varies from 1 to 0.6) coating can have a microhardness from 13.7 to 39.2 GPa (at the substrate temperature of 300–330°C). The pressure of the reactive gas directly affects the microhardness of monolayer coatings of the MN<sub>*x*</sub> type dur-

ing their formation. With increasing pressure of the reactive gas, the microhardness of the coatings increases, since the introduction of a larger volume of the reactive gas favors the more complete occurrence of plasma chemical reactions. But with a further growth of the pressure, the microhardness of the coating decreases because of the formation of coatings with an increased concentration of atoms of the reactive gas, which leads to an imperfection of the structure and to a decrease in the microhardness [16].

The X-ray diffraction studies of the phase composition of the coatings on Si substrates have shown the presence of a single phase, namely, titanium nitride with an fcc lattice. For all the samples there was observed a decrease in the lattice parameter as compared to the tabulated values for massive TiN. An analysis of the intensities of the diffraction lines depending on the deposition parameters (thickness of the coating, nitrogen flow rate, ion bombardment) demonstrates the domination of [111], [100], and [110] orientations in the coating texture. Figure 2 demonstrates X-ray diffraction patterns of coatings of different thickness produced under equal conditions. The estimation of the crystallite sizes from the widths of X-ray diffraction lines gives the average values from 10 to 20 nm.

It is usually assumed that upon plasma deposition of TiN coatings in vacuum compressive residual stresses are formed, the absolute value of which increases with increasing coating thickness. However, our results demonstrate that there exists a certain optimum thickness of the coating, at which the internal stresses in the coating are maximum. The dependences of residual stresses in the TiN coatings depending on thickness are shown in Fig. 3. As is seen, on substrates of both Si and AES the internal stresses have a maximum of about 5–7 GPa at the coating thickness of 900–950 nm (curves 1 and 2). Upon switching-on of an electromagnetic coil ( $I_C = 0.5 \text{ A}$ ), the density of the ion current at the substrate increases, which leads to a substantial growth of internal stresses (to 13 GPa, curve 3). In this case, the maximum of stresses also corresponds to the coating thickness of 900 nm.

The formation of residual stresses in TiN films deposited by magnetron sputtering appears to be not related to the difference of the thermal expansion coefficients of the film and substrate. An analysis of the substrate-temperature dependence on the time of deposition of the TiN coatings shown in Fig. 4 demonstrates that the method of magnetron sputtering provides a lower heat loading of the substrate in comparison with other vacuum-plasma techniques. Since in our experiments the temperature of the substrate did not exceed 100°C, the contribution of thermal stresses to residual stresses is negligibly small in comparison with the contribution of internal stresses that appear during the growth of the film. For example, on the silicon substrate ( $F_f = 300 \text{ GPa}$ ,  $\nu_{TiN} = 0.29$ ,  $\alpha_s = 4 \times 10^{-6} \text{ K}^{-1}$ ,  $\alpha_f = 9.4 \times 10^{-6} \text{ K}^{-1}$ ,  $T_D = 100^\circ\text{C}$ ,  $T_M = 20^\circ\text{C}$ ) the stresses in

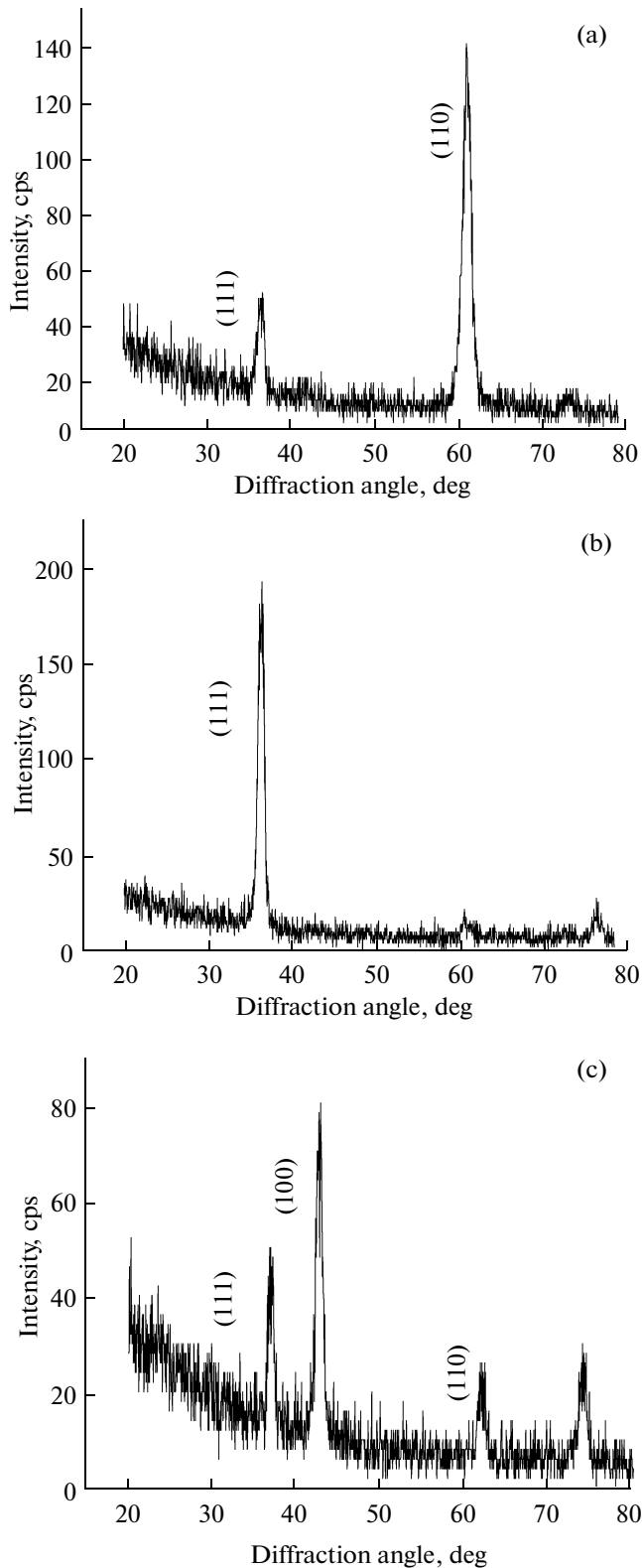


**Fig. 2.** X-ray diffraction patterns of TiN coatings ( $Q_{Ar} = 68 \text{ cm}^3/\text{min}$ ;  $Q_{N_2} = 16 \text{ cm}^3/\text{min}$ ; discharge power, 1.5 kW) with a thickness  $d$  equal to (a) 815, (b) 860, and (c) 1330 nm.

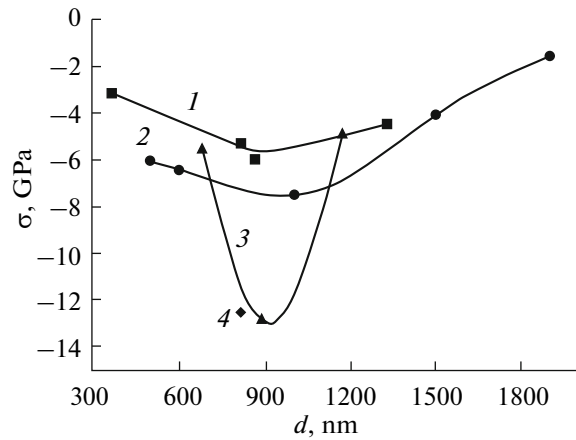


**Fig. 3.** Dependence of residual stresses  $\sigma$  in TiN films on their thickness  $d$  at different deposition parameters ( $Q_{Ar} = 68 \text{ cm}^3/\text{min}$ ;  $Q_{N_2} = 16 \text{ cm}^3/\text{min}$ ; discharge power, 1.5 kW): (1)  $I_c = 0 \text{ A}$ ,  $U_b = 0 \text{ V}$  (Si); (2)  $I_c = 0 \text{ A}$ ,  $U_b = 0 \text{ V}$  (AES); (3)  $I_c = 0.5 \text{ A}$ ,  $U_b = 0 \text{ V}$  (AES); (4)  $I_c = 0 \text{ A}$ ,  $U_b = -150 \text{ V}$  (AES). Curve 1 is for TiN on a Si substrate, and curves 2–4 are for TiN coatings on a substrate of electrical-sheet steel.

the coating calculated by formula (1) were tensile ( $\sigma_T = 182 \text{ Pa}$ ). On the AES substrates, which have a higher thermal expansion coefficient than that of the coating ( $\alpha_S = 11 \times 10^{-6} \text{ K}^{-1}$ ), the thermal stresses were compressive and were equal to  $-54 \text{ MPa}$ .

Therefore, it is the ion bombardment of the film surface during its growth that is responsible for the formation of large internal stresses in TiN coatings, which is confirmed by an increase in the level of stresses with increasing degree of magnetron imbalance.

The formation of residual stresses in thin films upon ion bombardment can be explained within the model of thermal spikes [17], which represent regions in which the energy of bombarding ions is transferred into the coating. The atoms of the coating acquire the energy of the bombarding ions through cascades of elastic collisions. As a result, they become more mobile and can move away from their initial positions.

An increase in the energy of bombarding ions lead to an increase in the volume of regions with an elevated temperature, which can be estimated as

$$V_{\text{spike}} = \frac{E}{\rho E_A}, \quad (6)$$

where  $E$  is the energy of a bombarding ion,  $\rho$  is the number of atoms in the volume of the coating, and  $E_A$  is an average activation energy required for displacing each atom in the thermal spike.

Calculations demonstrate that the temperature within these regions can achieve 5000 K [17]. The lifetime of thermal spikes is usually on the order of a few picoseconds.

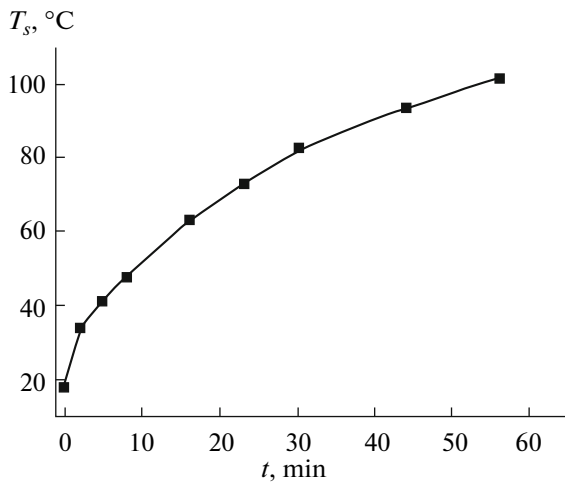


**Fig. 4.** Time dependence of the substrate temperature  $T_s$  during TiN film deposition ( $Q_{Ar} = 68 \text{ cm}^3/\text{min}$ ;  $Q_{N_2} = 16 \text{ cm}^3/\text{min}$ ; discharge power, 1.5 kW).

As a rule, the internal stresses upon ion bombardment are compressive and, with increasing energy of bombarding particles, their level first increases to a certain magnitude and then decreases [17]. The maximum corresponds to the energy of 100–200 eV.

As was shown in [18], with an increase in the bias voltage to about  $-150 \text{ V}$  the residual stresses in the coating increase. The size of TiN crystallites in this case decreases to 11–250 nm. The internal stresses are compressive and increase from about 1 GPa at  $U_b = 0 \text{ B}$  to 14 GPa at  $U_b = -150 \text{ V}$ . A further increase in  $U_b$  to above  $-150 \text{ V}$  is accompanied by a gradual decrease of compressive stresses to 5 GPa at  $U_b = -500 \text{ V}$ .

To estimate the energy of positive ions bombarding the surface of the growing film in the magnetron discharge, we have measured the energy spectra of ions in the reactive sputtering regime of the magnetron with switched-off ( $I_c = 0 \text{ A}$ ) and switched-on ( $I_c = 1 \text{ A}$ ) electromagnetic coil (Fig. 5).

The energy spectra of  $Ar^+$ ,  $N_2^+$ ,  $N^+$ , and  $Ti^+$  ions have maxima at the energy of about 2–4 eV, and also high-energy tails at the energy of 5–25 eV. The maximum corresponds to thermalized ions, whose energy is equal to the difference between the potential of the plasma and the anode potential. The presence of ions with an energy of up to 25 eV can be due to either neutralized ions reflected from the cathode or to gas atoms which gained their energy in collisions with sputtered atoms of the cathode. In both cases, the neutral atoms with a high energy were subsequently ionized in the plasma between the magnetic trap near the cathode surface and the substrate. The intensities of ion peaks increase by several times with an increase in the current in the coil from 0 to 1 A. The high-energy tail of Ti ions increases substantially with increasing  $I_c$ .

Thus, an increase in the current in the electromagnetic coil leads to a significant increase in the ion flux onto the bombarded substrate. In order to increase the energy of bombarding ions, pulses of negative bias with a frequency of 100 kHz and an amplitude of 150 V were applied to the substrate. This led to an increase in the hardness of TiN coating up to 29 GPa and an increase in internal stresses in the coating up to 13 GPa (point 4 in Fig. 3).

The growth of hardness can be induced by a refinement of the grain structure (the Hall–Petch rule) during additional ion bombardment upon applying negative bias pulses to the substrate [19]. This is testified by the images of the TiN films deposited at  $U_b = 0$  and  $-150 \text{ V}$  obtained with the help of atomic-force microscope (Fig. 6). In the absence of a bias voltage, the coatings have a columnar structure, which is common for magnetron sputtering, with a grain size to 100 nm (Fig. 6a). An increase in the energy of bombarding ions at the expense of the negative bias voltage applied to the substrate leads to the formation of a fine-grained structure of the coating with a low roughness of the surface (Fig. 6b).

Ion bombardment leads not only to a change in the level of internal stresses in the coating, but also to microstructure changes in the TiN coatings. The most frequently occurring orientations of crystals in TiN coatings are [111], [100], and [110]. It was demonstrated in many works that the preferred orientation varies from [100] to [111] upon an increase in the coating thickness.

As was shown in [16], TiN films deposited by vacuum arc sputtering with large compressive stresses have a [111] preferred orientation of crystallites, which changes to [100] at small compressive stresses. According to the model proposed by Pelleg et al. [20], these transformations are based on the mechanism of energy minimization in the coating. Therefore, below a certain level of internal stresses, the preferred orientation of grains in TiN coatings is [100], and above that level, [111] orientation prevails. Thus, the probability of formation of the film with a [111] orientation increases with increasing its thickness and internal stresses in it.

M.-J. Chou et al. [21] showed that the hardness of TiN coatings with a [111] preferred orientation is maximum. It can be explained by the fact that the level of stresses in such coatings is largest and that, as is well known, materials with high internal stresses demonstrate the maximum hardness [22].

Our results are in good agreement with the above-mentioned literature data (see Table 1). It has been shown that internal stresses in the coating increase with increasing both ion flux onto the substrate (with increasing degree of magnetron imbalance) and with increasing energy of these ions (with applying a negative bias voltage to the substrate). The thickness of the coating also is not the least of the factors.

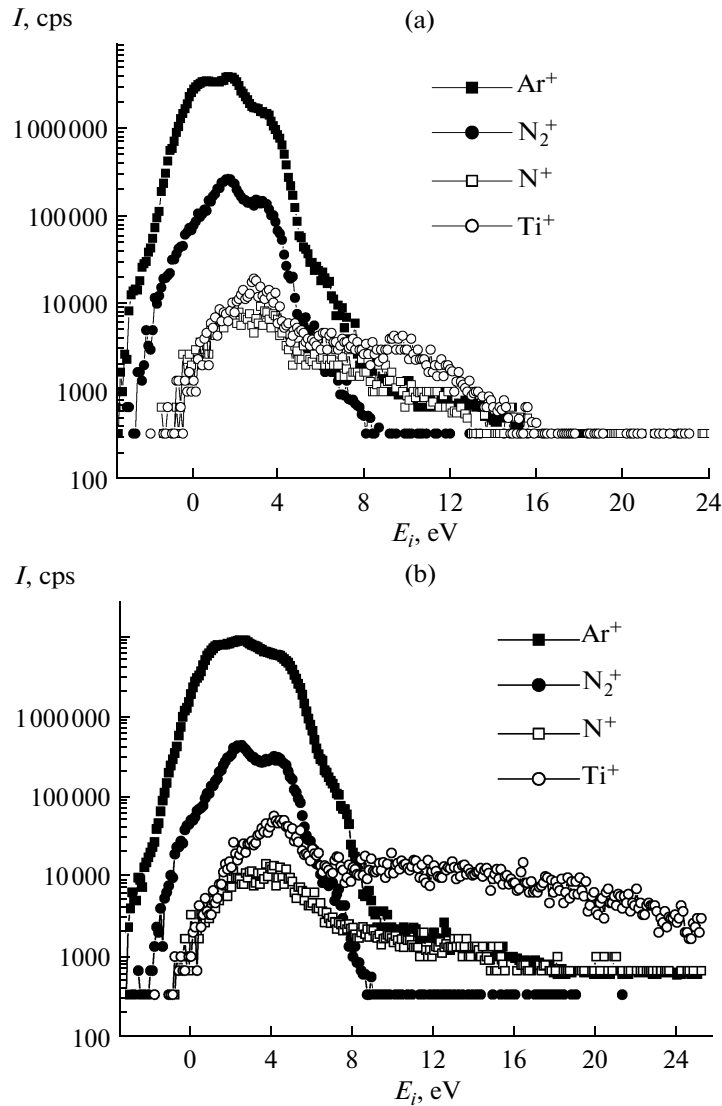


**Fig. 5.** Energy spectra of ions in the magnetron discharge at different current in the electromagnetic coil ( $P_{Ar} = 0.38$  Pa,  $P_{N_2} = 0.07$  Pa): (a)  $I_c = 0$  A,  $U_d = 312$  V,  $I_d = 3$  A,  $P_d = 0.9$  kW; and (b)  $I_c = 1$  A,  $U_d = 364$  V,  $I_d = 3$  A,  $P_d = 1.1$  kW.

Then, we have studied the dependence of specific power losses in samples of the AES of grade 3405 with TiN coatings on the thickness of these coatings and deposition parameters (Table 2).

In the untreated samples of the 3405 electrical steel 0.35 mm thick with a commercial insulation coating, the specific losses of power were 1.47 W/kg. Before depositing nitride coatings, the insulating coating was etched away in an aqueous solution of HCl, after which the sample was mechanically polished to a mirror finish. The thickness of the sample was reduced to 0.33 mm. After such treatment, the specific energy losses in the samples increased to 1.62 W/kg. As is seen from Table 2, the specific losses in the samples with TiN coatings depend on the thickness of the coating, just as the internal stresses in the coatings do. This is

confirmed by the fact that the coatings with high residual stresses deposited onto the electrical steel are capable to influence the specific energy losses in it. The maximum decrease in the specific losses is observed at the coating thickness of 800–900 nm, i.e., in the case where the internal stresses are maximum (see Fig. 3).

The maximum decrease in the specific losses was achieved in the samples 10C and 11C, on which the coatings were deposited simultaneously with applying a negative bias voltage to the substrate. In these samples the specific energy losses  $P_{1.7/50}$  were decreased to 1.27 W/kg, i.e., by about 15%.

Like the authors of [23], we relate a decrease in the specific magnetic losses to the formation of compressive stresses in a thin surface layer of the material, which lead to the formation of a typical fine-grained

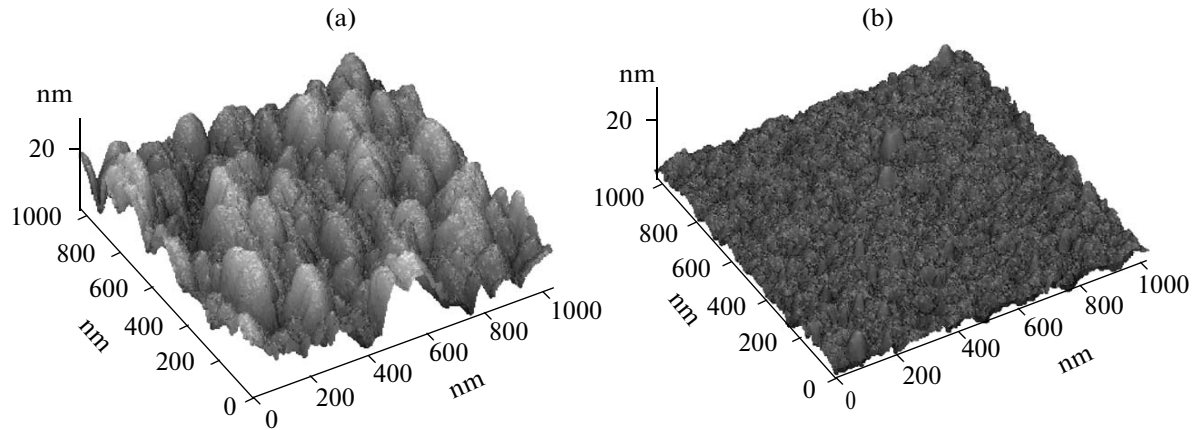


**Fig. 6.** Images of the surface of TiN coatings on Si obtained (a) without a bias voltage ( $Q_{Ar} = 68 \text{ cm}^3/\text{min}$ ,  $Q_{N_2} = 16 \text{ cm}^3/\text{min}$ ,  $I_c = 0$ ,  $U_b = 0$ ,  $d = 860 \text{ nm}$ ) and (b) with a negative bias voltage ( $Q_{Ar} = 68 \text{ cm}^3/\text{min}$ ,  $Q_{N_2} = 16 \text{ cm}^3/\text{min}$ ,  $I_c = 0$ ,  $U_b = -150 \text{ V}$ ,  $d = 815 \text{ nm}$ ).

surface structure of magnetic domains and a multilayered domain structure over the sample cross section, to a refinement of the main domains, and to peculiarities of the domain dynamics upon magnetization reversal, which affect the formation of magnetization reversal centers and the velocity of motion of domain walls. A decrease in the velocity of domain walls at the surface of a material with a TiN coating induced by the stressed state of thin surface layers can result in changes in the curvature of domain walls (over the cross section of the material) and in a decrease in their average velocity of motion.

An analysis of the domain structure and orientation relative to the easy axis was beyond the scope of this study. However, it is known from the literature that the maximum decrease in magnetic losses is provided by creating a magnetic structure in the form of narrow transversely oriented  $180^\circ$  domains. Such a structure

formed on a silicon iron under the effect of compressive stresses oriented along the [001] direction was observed in [23].

## CONCLUSIONS

As a result of experiments on applying TiN coatings onto electrical-sheet steel with a help of a magnetron sputtering system with an electromagnetic coil, it has been shown that the residual stresses in the coatings deposited with ion assistance depend on the thickness of the coating and the flux and energy of the bombarding ions. The effect of the parameters of deposition of TiN coatings on the level of the internal stresses that are formed in them has been studied. The fact that the application of coatings with high residual stresses allows reducing specific losses in the electrical-sheet steel has been testified. The optimum regimes of dep-

**Table 2.** Dependence of specific energy losses  $P_{1.7/50}$  in the samples of electrical-sheet steel on the thickness  $d$  of TiN coatings obtained at different currents  $I_c$  in the disbalancing coil and different bias voltages  $U_b$  ( $Q$  is the gas flow rate; the discharge power is 1.5 kW)

No.	$Q_{Ar}$ , $\text{cm}^3/\text{min}$	$Q_{N_2}$ , $\text{cm}^3/\text{min}$	$I_c$ , A	$U_b$ , V	$d$ , nm	$P_{1.7/50}$ , W/kg
1C	68	16	0	0	600	1.77
2C	68	16	0	0	1000	1.4
3C	68	16	0	0	1500	1.51
4C	68	16	0.5	0	680	1.7
5C	68	16	0.5	0	880	1.47
6C	68	16	0.5	0	1170	1.69
10C	68	16	0	-100	810	1.27
11C	68	16	0	-150	800	1.27



osition of TiN coatings with residual stresses reaching 13 GPa, high hardness, and good adhesion to a substrate have been found. The application of such coatings allows reducing specific energy losses in electrical steel by 15%.

#### ACKNOWLEDGMENTS

This work was supported by the Federal Agency on Science and Innovations (Federal contract no. 02.516.11.6117).

#### REFERENCES

1. S. V. Kayukov, E. G. Zaichikov, I. A. Dudorov, et al., "Optimization of Laser Treatment Regimes of Anisotropic Electrotechnical Steel," *Izv. Samar. Nauch. Tsentr. RAN* **5** (1), 66–73 (2003).
2. B. K. Sokolov, V. V. Gubernatorov, Yu. N. Dragoshanskii, and B. P. Yatsenko, "Laser Treatment of Electrotechnical Materials," *Stal'*, No. 5, 63–66 (1996).
3. I. K. Schastlivtseva, L. B. Kazadzhan, B. K. Sokolov, et al., "Influence of Shape and Grain-Size on Magnetic Properties of Textured Transformer Steel," *Fiz. Met. Metalloved.*, No. 3, 542–548 (1976).
4. G. S. Korzunin, V. K. Chistyakov, Yu. N. Dragoshanskii, et al., "Effect of Electro-Insulating Coatings on the Anisotropy of Magnetic Characteristics of Textured Electrical-Sheet Steel," *Defektoskopiya*, No. 8, 34–46 (2000).
5. G. S. Korzunin, I. P. Sysolyatina, and V. K. Chistyakov, "Effect of the Distribution of Chemical Elements in Insulating Coatings and Surface Layers of Electrical-Sheet Steel on Its Magnetic Properties," *Fiz. Met. Metalloved.* **95** (6), 1–7 (2003) [*Phys. Met. Metallogr.* **95** (6), 544–550 (2003)].
6. F. Brailsford and Z. H. M. Abu-eid, "Effect of Tensile Stress on the Magnetic Properties of Grain-Oriented Silicon-Iron Lamination," *Proc. Inst. Electr. Engrs* **110** (4), 751–757 (1963).
7. B. Schuhmacher, K. Guenther, H. Hingmann, et al., "Grain-Oriented Magnetic Steel Sheet Comprising an Electrically Insulating Coating," US Patent, 7169479 (2007).
8. M. Bielawski, "Residual Stress Control in TiN/Si Coatings Deposited by Unbalanced Magnetron Sputtering," *Surf. Coat. Technol.* **200**, 3987–3995 (2006).
9. H. Yamaguchi, M. Muraki, and M. Komatsubara, "Application of CVD Method on Grain-Oriented Electrical Steel," *Surf. Coat. Technol.* **200**, 3351–3354 (2006).
10. E. Mounier and Y. Pauleau, "Effect of Energetic Particles on the Residual Stresses in Nonhydrogenated Amorphous Carbon Films Deposited on Grounded Substrates by DC Magnetron Sputtering," *J. Vac. Sci. Technol., A* **14** (4), 2535–2543 (1996).
11. A. A. Solov'ev, N. S. Sochugov, K. V. Oskomov, and S. V. Rabotkin, "Investigation of Plasma Characteristics in an Unbalanced Magnetron Sputtering System," *Fiz. Plazmy* **35** (4), 1–10 (2009) [*Plasma Phys. Rep.* **35**, (5) 399–408 (2009)].
12. M. L. Trunov, A. G. Anchugin, N. D. Savchenko, and Yu. Yu. Firtsak, "Control of Internal Stresses in Vacuum-Precipitated Films," *Vacuum. Tekh. Tekhnol.* **1** (5–6), 12–21 (1991).
13. L. Shuangbiao and Q. J. Wang, "Determination of Young's Modulus and Poisson's Ratio for Coatings," *Surf. Coat. Technol.* **201** (14), 6470–6477 (2007).
14. B. U. Asanov and V. P. Makarov, "Nitride Coatings Obtained by Vacuum-Arc Scattering," *Vestn. Kirg.-Ross. Slav. Univ. (KRSU)*, **2** (2), 1–3 (2002).
15. P. H. Mayrhofer, F. Kunc, J. Musil, and C. Mitterer, "A Comparative Study on Reactive and Non-Reactive Unbalanced Magnetron Sputter Deposition of TiN Coatings," *Thin Solid Films* **415**, 151–159 (2002).
16. A. V. Belyi, G. D. Karpenko, and N. K. Myshkin, *Structure and Methods of Formation of Wear-Resistant Surface Sheets* (Mashinostroenie, Moscow, 1991) [in Russian].
17. M. M. M. Bilek, D. R. McKenzie, and W. Moeller, "Use of Low Energy and High Frequency PBII during Thin Film Deposition to Achieve Relief of Intrinsic Stress and Microstructural Changes," *Surf. Coat. Technol.* **186**, 21–28 (2004).
18. Z. Soukup, J. Lhotka, J. Musil, and D. Rafaja, "Effect of Ti Interlayer and Bias on Structure and Properties of TiN Films," *Czechoslovak J. Phys.* **50** (5), 655–663 (2000).
19. V. M. Shulaev, A. A. Andreev, V. F. Gorban', and V. A. Stolbovoi, "Comparison of Characteristics of Vacuum-Arc Nanostructured TiN Coatings Precipitated by High-Voltage Pulses upon Substrate," *Fiz. Inzhen. Poverkhn.* **94** (1–2), 94–97 (2007).
20. J. Pelleg, L. Z. Zevin, and S. Lungo, "Reactive-Sputter-Deposited TiN Films on Glass Substrates," *Thin Solid Films* **197**, 117–128 (1991).
21. M.-J. Chou, G.-P. Yu, and J.-H. Huang, "Mechanical Properties of TiN Thin Film Coatings on 304 Stainless Steel Substrates," *Surf. Coat. Technol.* **149**, 7–13 (2002).
22. P. Martin, A. Bendavid, and T. Kinder, "The Deposition of TiN Thin Films by Filtered Cathodic Arc Techniques," *IEEE Trans. Plasma Sci.* **25** (4), 675–679 (1997).
23. B. K. Sokolov, V. V. Gubernatorov, Yu. N. Dragoshanskii, et al., "Effect of Ion-Beam Treatment on the Magnetic Properties of Soft Magnetic Materials," *Fiz. Met. Metalloved.* **89** (4), 32–42 (2000) [*Phys. Met. Metallogr.* **89** (4), 348–357 (2000)].